Journal of the European Ceramic Society **16** (1996) 929–935

S0955-2219(96)00019-2
0955-2219/96/$15.00

The Use of Lithium as a Dopant in the Directed Melt Oxidation of Aluminium

X. Gu & R. J. Hand*

Department of Engineering Materials, University of Sheffield, Sir Robert Hadfield Building, Mappin Street, Sheffield S1 3DJ, UK

(Received 12 October 1995; revised version received 21 December 1995; accepted 3 January 1996)

Abstract

A Li source has been used to initiate directed melt oxidation of Al; the Li source used was Li_2CO_3. Growth both into free space, in which case Li_2CO_3 powder was placed on the metal surface, and into preform bodies comprising pure particulate α-Al_2O_3 mixed with a doping amount of Li_2CO_3, has been examined. In both cases it is shown that Li may initiate the directed oxidation reactions in the absence of any other dopants and that Li is therefore an effective dopant for the production of Al_2O_3/Al by the directed melt oxidation process. The products were characterized using scanning electron microscopy, transmission electron microscopy and X-ray diffraction. A cyclic reaction sequence for Al_2O_3/Al composite growth in the Li-doped system is postulated. This process is initiated by the formation of $LiAl_5O_8$ which aids the breakdown of the stable oxide film that would normally form on aluminium in a similar fashion to magnesium aluminium spinel in the Mg-doped system. The process involves motion of Li from within the growth to the reaction front; this can occur because of the high vapour pressure of Li at the reaction temperature. The effects of the preform body on these cyclic reactions are also considered.

Introduction

The directed melt oxidation process involves the directed growth of a composite product from a bulk molten metal via oxidation of the melt by a vapour-phase oxidant (e.g air).[1] This composite comprises an interconnected ceramic reaction product and, usually, several per cent of residual metal. The product may be shaped by growing the product either into a defined empty space or into a shaped region containing a preform comprising a loosely packed filler, ceramic fibres or whiskers. In this paper we distinguish the two cases by referring to bodies produced by growth into free space as 'unreinforced bodies' and to ones produced by growth into a preform body as 'reinforced bodies'.

The growth of products by directed melt oxidation depends crucially on the presence of dopants, which initiate and maintain the process. These dopants may be introduced by alloying with the pure parent metal or externally in the form of elemental or oxide powders.

Much of the published literature on this process has used alloys to introduce the doping elements. For example, growth of Al_2O_3/Al composites from Al alloys containing Mg either alone or in conjunction with Si has been studied by several authors.[1–3] More recently, the use of external doping with Mg or MgO powders has received some attention.[4,5]

It has been shown that Mg, either in elemental form or as part of a compound, can initiate directed melt oxidation reactions in the Al_2O_3/Al system. For example, Xiao and Derby[4] have shown that MgO may be used as an external dopant to initiate growth with pure Al, and that oxide growth occurs in the temperature range 1100–1400°C, with no incubation period. Our previous work,[5] in which Mg powder was used as external dopant for directed oxidation of pure Al, also showed that only Mg is necessary to initiate and sustain the reaction growth. Mg can initiate growth in the Al_2O_3/Al system as it promotes the formation of a non-protective oxide layer at the interface between the growth oxide and oxidant. This layer plays an important role in the subsequent directed oxidation cyclic reaction sequence. By comparison Si seems only to accelerate the reaction process, probably by modifying the viscosity of the aluminium melt.[2] Na and Sn have also been examined as possible dopants; Na can initiate the process although it leads to low quality products and Sn apparently has similar effects to Si.

In the current work we have examined the possibility of using Li to initiate directed melt oxidation growth in the Al_2O_3/Al system. Li was chosen

*To whom correspondence should be addressed.

as a potential dopant because examination of the periodic table reveals that, in general, on moving diagonally across the periodic table the elements have certain similarities. This is because as one moves across a period, the charge on the ions increases and the size decreases, causing the polarizing powder to decrease, whereas on moving down a group, the size increases and polarizing power increases. On moving diagonally these two effects partly cancel each other, so that there is no marked change in properties. The type and strength of bond formed and the properties of the compounds are therefore often similar, although the valency is different. The similarities between diagonally related pairs of elements are usually weaker than those within a group, but they are quite pronounced for the following pairs of elements.[6] Li and Mg; Be and Al; B and Si. Therefore, there are some similarities in the properties of Mg and Li which were expected to allow Li to be used as dopant in directed oxidation of aluminium; in particular, both Mg and Li have very high vapour pressures at high temperature and they both form spinel structures with Al_2O_3.

In this paper the use of Li_2CO_3 as an externally applied lithium source in the directed melt oxidation of aluminium has been examined. Both unreinforced and α-Al_2O_3 particulate-reinforced bodies have been produced. In both cases, a detailed description of the microstructure is provided.

Experimental Procedure

A block of 99·8% pure Al (Alcan) was placed in a cavity shaped in an alumina crucible using fine alumina powder. Between 1·25 and 7·50 wt% (based on the weight of Al) reagent grade Li_2CO_3 powder (Fisons) was either applied directly on the surface of the Al block for composites grown into free space, or mixed with fine pure α-Al_2O_3 (A17, Alcoa) for composites grown into a preform body. The respective experimental arrangements are given in Figs 1(a) and 1(b).

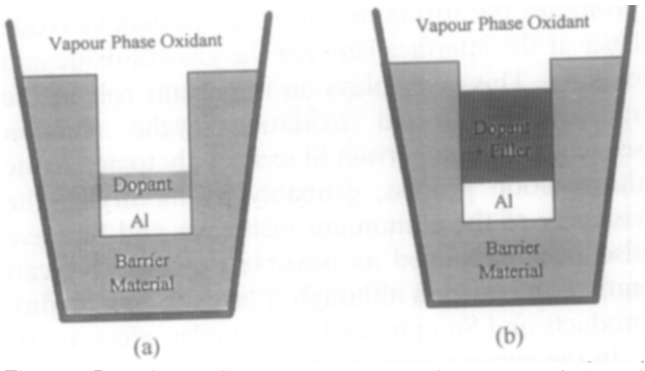

Fig. 1. Experimental arrangements used. (a) Unreinforced bodies: dopant directly placed on the Al block. (b) Reinforced bodies: dopant mixed with filler and the mixture placed above the Al block.

The prepared systems were heated in air at 200°C h^{-1} in a muffle furnace to a soaking temperature of 700, 900 or 1180°C. Samples fired to 700 and 900°C were held at these temperatures for 3 h, whereas samples fired to 1180°C were held at this temperature for 35 h. In all cases the samples were cooled to room temperature inside the furnace.

Fired samples were sectioned parallel or perpendicular to the growth direction and the different regions analysed by qualitative X-ray diffraction. These samples were subsequently mounted in epoxy resin, ground and diamond polished to 1 μm, before carbon coating for examination using scanning electron microscopy (SEM; Jeol JSM 6400) and energy dispersive spectroscopy (EDS; Link Analytical 6276). For transmission electron microscopy (TEM), the samples were punched to 3 mm discs, mechanically thinned to around 20 μm, ion milled at 6·0 keV until perforation, coated with carbon, and examined in a Philips EM420 at 100 keV.

Results

Growth into free space

Small, soft, black compacts were produced when samples containing 2·47 or 7·41 wt% Li_2CO_3 were fired to 700°C for 3 h. XRD (Fig. 2) showed that these compacts consisted of Al, Li_2CO_3, α-$LiAlO_2$,

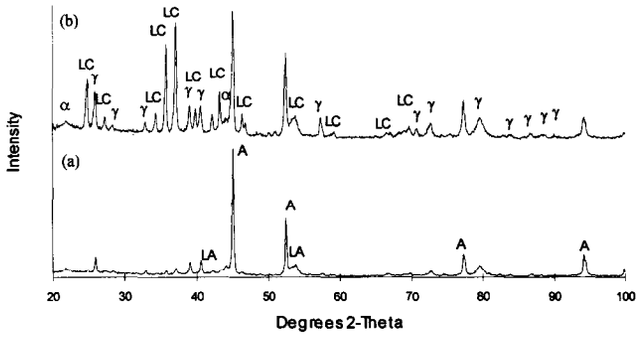

Fig. 2. XRD traces of samples fired for 3 h at 700°C: (a) Al–2·47 wt% Li_2CO_3; (b) Al–7·41 wt% Li_2CO_3 (A, Al; LC, Li_2CO_3; α, α-$LiAlO_2$; γ, γ-$LiAlO_2$; LA, $LiAl_5O_8$).

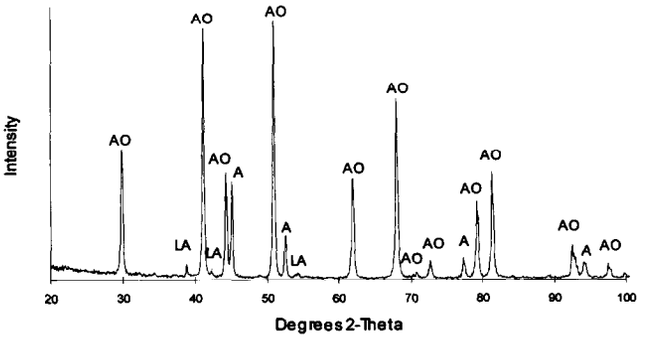

Fig. 3. XRD trace of Al–1·23 wt% Li_2CO_3 sample fired for 35 h at 1180°C (A, Al; AO, Al_2O_3; LA, $LiAl_5O_8$).

γ-$LiAlO_2$ and $LiAl_5O_8$, and that, within the limits of detection, no Al_2O_3 had been produced.

In samples doped with 1·23 wt% Li_2CO_3 and fired at 1180°C, Al_2O_3/Al growth was obtained; the Al block was totally exhausted after a soaking time of 35 h. Growth proceeded not only upwards from the top surface of the Al block but sideways into the barrier material. A section cut parallel to the growth was analysed by XRD which showed (Fig. 3) that the product was mainly Al and α-Al_2O_3; in addition, a small amount of $LiAl_5O_8$ was detected. Cross-sections of the growth product were also analysed by SEM. At the top of the sample there was a thick layer comprising Al pockets within a ceramic matrix (Fig. 4). Beneath this thick layer there was a series of thinner alternating dense and less dense layers (Fig. 5). The dense layers contained Al channels and the less dense ones contained no Al. In the centre of this sample (Fig. 6), an interconnected matrix was obtained. At the bottom of the sample (Fig. 7), further alternating dense and less dense layers were found. In addition, in the base of the product, the presence of Li-containing phases can be inferred from the backscattered electron image, as well as a small amount of AlN, which was identified by EDS (Fig. 8). Around the outermost surface of these samples, a thin Li-containing layer was observed (Fig. 9).

Although it is very difficult to identify the ceramic oxide as Al_2O_3 or $LiAl_5O_8$ using EDS since lithium

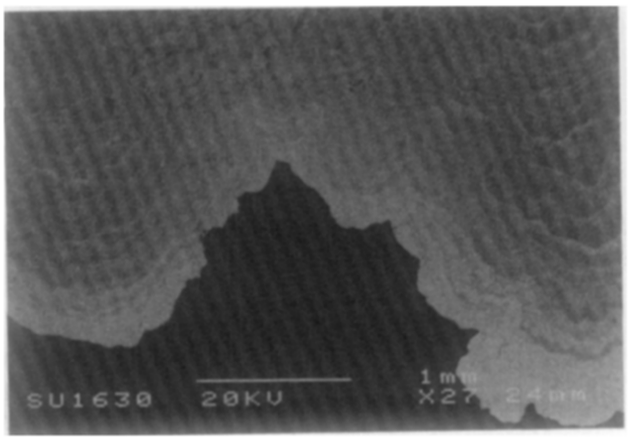

Fig. 4. SEM micrograph of the Al–1·23 wt% Li_2CO_3 sample fired to 1180°C for 35 h, showing a thick matrix layer at the top.

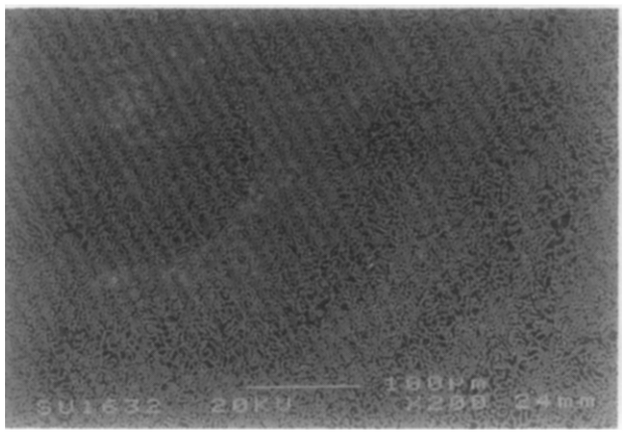

Fig. 5. SEM micrograph of the Al–1·23 wt% Li_2CO_3 sample fired to 1180°C for 35 h, showing alternating dense and less dense layers.

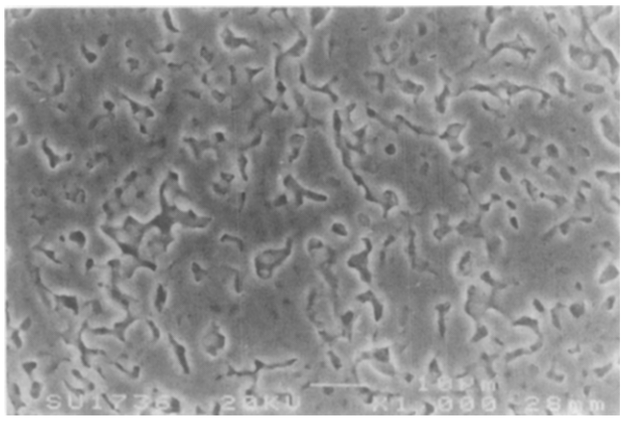

Fig. 6. SEM micrograph of the Al–1·23 wt% Li_2CO_3 sample fired to 1180°C for 35 h, showing interconnected Al_2O_3/Al matrix in the centre region.

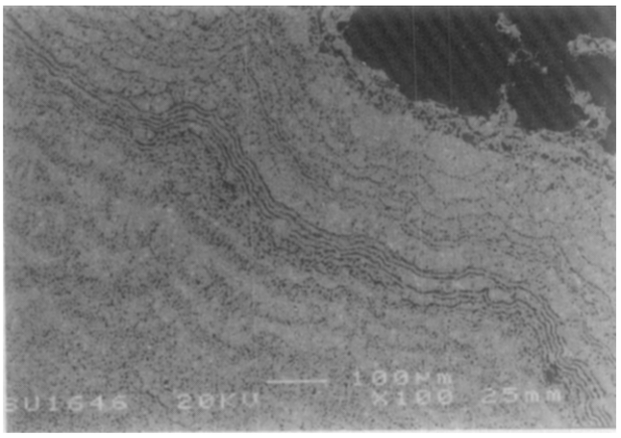

Fig. 7. SEM micrograph of the Al–1·23 wt% Li_2CO_3 sample fired to 1180°C for 35 h, showing alternating dense and less dense layers at the bottom of the product.

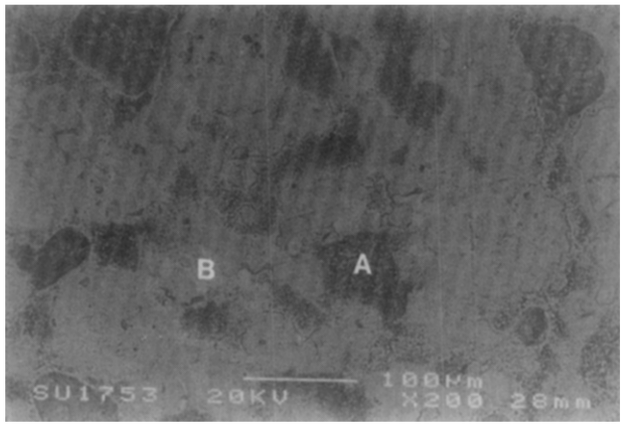

Fig. 8. Backscattered electron image of the Al–1·23 wt% Li_2CO_3 sample fired to 1180°C for 35 h, showing a Li-containing phase (dark feature — A) and AlN (light feature — B).

is too light, TEM showed up differences between these two phases. High-angle $LiAl_5O_8$–$LiAl_5O_8$ grain boundaries were commonly observed (Fig. 10), which was similar to the high-angle $MgAl_2O_4$–$MgAl_2O_4$ grain boundaries reported by Breval *et al.* on the Mg-doped system.[7] It was also found that many

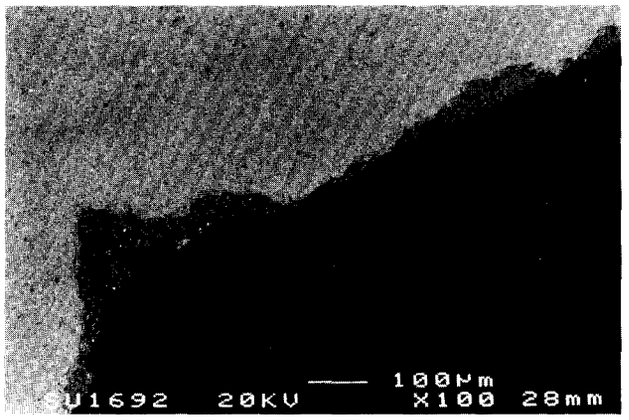

Fig. 9. SEM micrograph of the surface of a sample fired to 1180°C for 35 h, showing a thin, Li-containing layer on the surface.

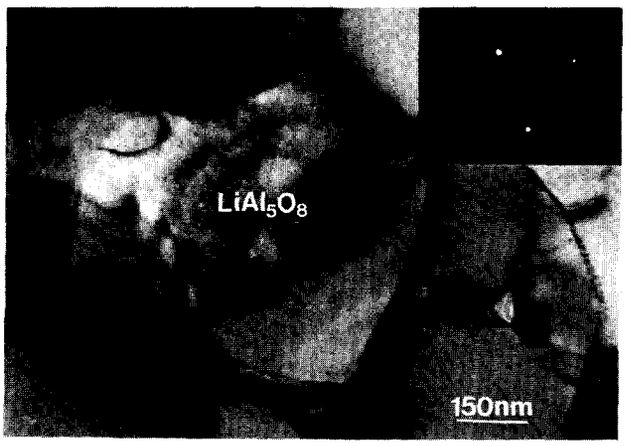

Fig. 10. TEM micrograph of a $LiAl_5O_8$ feature showing a high-angle $LiAl_5O_8$–$LiAl_5O_8$ grain boundary. Diffraction pattern shows $LiAl_5O_8$ [1 9 $\bar{2}$ $\bar{3}$].

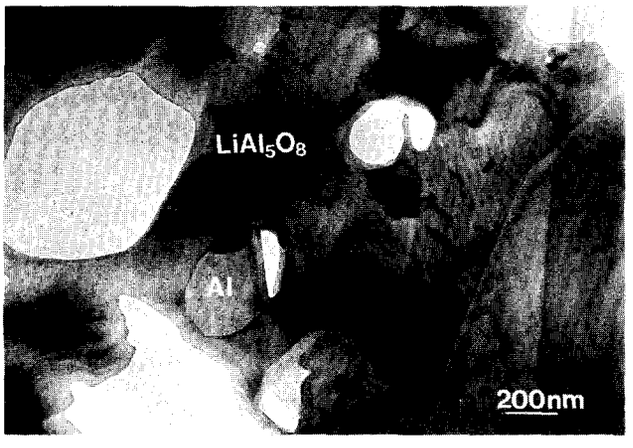

Fig. 11. TEM micrograph showing inclusions of Al within $LiAl_5O_8$ matrix.

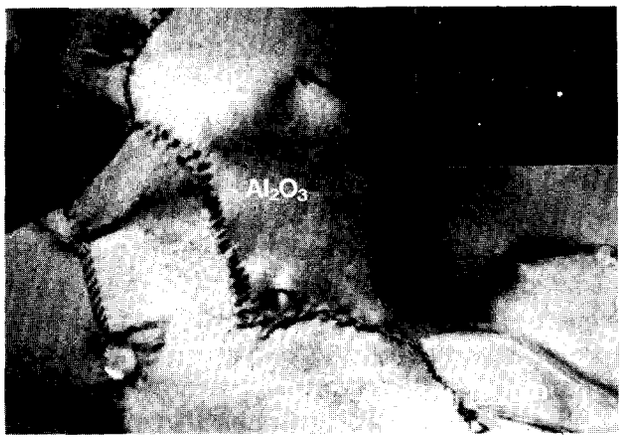

Fig. 12. TEM micrograph of Al_2O_3 feature showing low-angle Al_2O_3–Al_2O_3 grain boundary and high-angle Al_2O_3–Al grain boundary. Diffraction pattern shows Al_2O_3 [00$\bar{6}$].

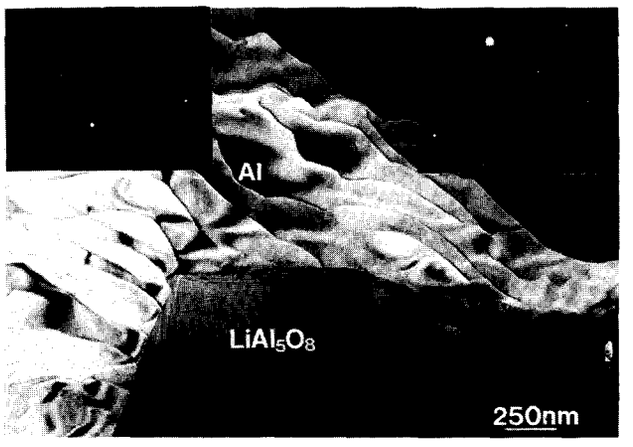

Fig. 13. TEM micrograph showing Al channel between $LiAl_5O_8$ crystals. Diffraction patterns show Al [0 $\bar{1}$ 3] (right) and $LiAl_5O_8$ [0 4 $\bar{3}$] (left).

inclusions of unoxidized Al remained within the $LiAl_5O_8$ matrix (Fig. 11). Low-angle grain boundaries were observed between Al_2O_3 grains (Fig. 12) and Al pockets were found set in the Al_2O_3–Al_2O_3 grain boundaries with a high-angle Al–Al_2O_3 phase boundary. This was also in agreement with the features seen in the directed melt oxidation of Al–Mg alloys.[1,3,7] Some thin channels of aluminium were also found (Fig. 13), which separate neighbouring $LiAl_5O_8$ crystals rather than Al_2O_3 crystals reported in the Mg-doped system by Newkirk *et al.*[1]

Growth into a preform body

Apart from a small amount of surface oxidation of the aluminium blocks, no growth was found in samples containing either 2·47 or 7·41 wt% Li_2CO_3 that had been heated to 900°C for 3 h. XRD showed, however (Fig. 14), that after firing the filler powder mixture consisted of α-Al_2O_3, α-$LiAlO_2$, γ-$LiAlO_2$ and $LiAl_5O_8$. The greater the initial Li_2CO_3 content, the more γ-$LiAlO_2$ was obtained in the fired mixture.

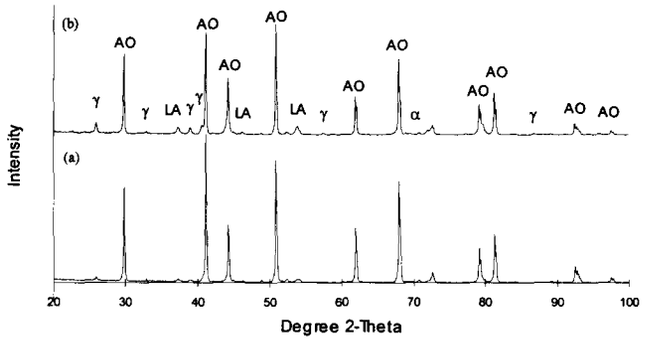

Fig. 14. XRD traces of Al_2O_3 particle-reinforced samples fired for 3 h at 900°C: (a) Al–2·47 wt% Li_2CO_3; (b) Al–7·41 wt% Li_2CO_3 (A, Al; α, α-$LiAlO_2$; γ, γ-$LiAlO_2$; LA, $LiAl_5O_8$).

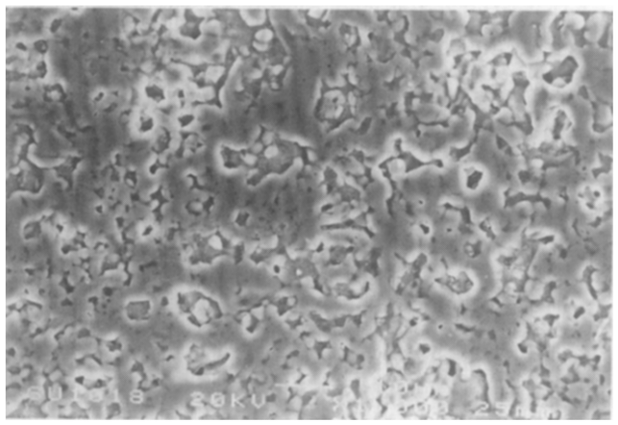

Fig. 15. SEM micrograph of Al_2O_3 particle-reinforced Al–1·23 wt% Li_2CO_3 sample fired to 1180°C for 35 h.

In systems doped with between 1·24 and 7·41 wt% Li_2CO_3 that had been heated to 1180°C for 24 or 35 h, irregular growths were obtained in the lower part of the dopant/filler mixture and part of the aluminium block was consumed. On inspection of the cross-section, it was difficult to distinguish between alumina filler and growth. The section was analysed by XRD which showed that although $LiAl_5O_8$ was present in addition to α-Al_2O_3 and Al, no $LiAlO_2$ was present. The fired mixture above the growth product consisted of α-Al_2O_3 (filler) and $LiAl_5O_8$. Unlike the unreinforced body, there were no alternating dense/less dense layers within the micro-structure of the reinforced body. A lithium aluminate phase was concentrated on the surface of the product body and, within the growth, an interconnected Al_2O_3/Al matrix that contained filler Al_2O_3 particles (0·3 μm diameter) and unoxidized Al channels was formed (Fig. 15).

Discussion

Ginsberg and Datta[8] claimed that lithium confers a greater reactivity to aluminium melt than any other alloying element. Small amounts of lithium (3 wt%) dramatically alter the nature of the molten alloy to the extent that traditional materials of construction used in the melting and transfer of aluminium alloy are rendered inadequate. Furthermore, rapid reaction of lithium with oxygen and water from the ambient atmosphere renders the oxide crust that forms on the molten metal non-protective, leading to severe volatilization of lithium, necessitating processing under an inert atmosphere. This removal of coherent film from the molten alloy also allows intimate contact with particles and promotes wetting and infiltration.[9]

Butler and co-workers[10,11] showed that a binary Al–3 wt% Li alloy developed surface films of spinel oxides such as $LiAl_5O_8$ and γ-$LiAlO_2$ in oxygen-containing environments around 500°C. Under pure oxygen γ-$LiAlO_2$ and α-Al_2O_3 developed at around 700°C on alloys containing relatively low levels of Li. X-ray analysis[12] of oxide films grown in air at 750°C on Al–0·3 wt% Li and Al–1·2 wt% Li indicated that γ-AL_2O_3 was present in addition to γ-$LiAlO_2$. Field and co-workers[11,13] studied the oxidation of liquid Al–3 wt% Li alloy under different environments. In dry air the oxidation sequence with increasing temperature was $Li_2O \rightarrow Li_2CO_3 \rightarrow$ γ-$LiAlO_2$. In wet air, Li_2O and Li_2CO_3 were stable up to 500°C but above this temperature a mixture of cubic spinel $LiAl_5O_8$ and $LiAlO_2$ existed. The surface of molten Al–3 wt% Li appeared to behave chemically like pure lithium and thus Al played only a minor role during oxidation. Oxidation was not limited by Li diffusion but controlled by the nucleation and growth of crystalline reaction products at the metal–oxide interface.

In this work, pure aluminium and an external Li_2CO_3 dopant, rather than an Al–Li alloy, have been used. XRD of Li_2CO_3 fired at 600°C, and DTA traces of Li_2CO_3 heated from room temperature to 1180°C, show that Li_2CO_3 is very stable even above 660°C (the melting point of aluminium) and that the decomposition reaction occurs around 730°C. Thus, in the directed melt oxidation process below 730°C, Li_2CO_3 may react directly with the protective Al_2O_3 oxide layers that will be present on the pure aluminium:

$$Li_2CO_3 + Al_2O_3\ (\text{film}) \rightleftharpoons 2LiAlO_2 + CO_2 \quad (1)$$

or

$$Li_2CO_3 + 5Al_2O_3\ (\text{film}) \rightleftharpoons 2LiAl_5O_8 + CO_2. \quad (2)$$

These reactions can aid the breakdown of stable oxide film in a similar fashion to magnesium aluminate spinel, $MgAl_2O_4$, in the Mg-doped system.[5]

On the other hand, above the melting point of aluminium, molten aluminium may also react directly with Li_2CO_3 to form $LiAl_5O_8$ or $LiAlO_2$, i.e.

$$4Al + 2Li_2CO_3 + 3O_2 \rightleftharpoons 4LiAlO_2 + 2CO_2 \quad (3)$$

$$20Al + 2Li_2CO_3 + 15O_2 \rightleftharpoons 4LiAl_5O_8 + 2CO_2. \quad (4)$$

As Li_2O is never observed it is thought that these reactions occur preferentially to the high-temperature decomposition of the carbonate to the oxide.

Lithium aluminates are therefore formed on the surface of the parent metal and aluminium liquid continues to penetrate this lithium aluminate layer by capillary action and react with lithium aluminates. Byker *et al.*[14] claimed that $LiAl_5O_8$ spinel is stable over a substantial range of stoichiometry and thus any $LiAlO_2$ could be transformed to $LiAl_5O_8$ on contact with excess Al:

$$LiAlO_2 + 4Al + 3O_2 \rightleftharpoons LiAl_5O_8. \quad (5)$$

$LiAl_5O_8$ can also react with liquid Al to produce Al_2O_3

$$LiAl_5O_8 + Al \rightleftharpoons 3Al_2O_3 + Li \quad (6)$$

The resulting Li vaporizes easily to the reaction front and would reform $LiAl_5O_8$ again producing the Li-rich layer seen on the outermost surface of the products:

$$Li + 5Al + 4O_2 \rightleftharpoons LiAl_5O_8. \quad (7)$$

This cycle of oxidation reactions leads to the directed oxidation Al_2O_3/Al body growth although some Li may be lost to the environment.

As the lithium aluminate layer is constantly being broken down and reformed, the orientation of lithium aluminate grains formed at a later time is not related to those formed earlier. High-angle grain boundaries are therefore observed in the lithium aluminate layer (Fig. 10). By comparison, after the initial development of an Al_2O_3 layer there is always Al_2O_3 present in the system. Hence the orientation of subsequently grown Al_2O_3 is related to the pre-existing Al_2O_3 grains, and low-angle grain boundaries are seen between Al_2O_3 grains (Fig. 12).

Within the base of growth product the oxygen content may be exhausted so that the remaining Al liquid may react with nitrogen (present in air which was used as the oxidizing atmosphere) to form AlN.[5]

In the Al_2O_3/Al growth into a preform body, fine Al_2O_3 particles were used as filler. Before the directed melt oxidation reactions started, the following reactions between Al_2O_3 filler and Li_2CO_3 would occur:

$$Li_2CO_3 + Al_2O_3 \text{ (filler)} \rightleftharpoons 2LiAlO_2 + CO_2 \quad (8)$$

and

$$Li_2CO_3 + 5Al_2O_3 \text{ (filler)} \rightleftharpoons 2LiAl_5O_8 + CO_2. \quad (9)$$

When aluminium liquid infiltrates into the mixture of dopant and reinforcement, $LiAlO_2$ leads to breakdown of the Al_2O_3 protective layer on the aluminium surface by the following reaction:

$$LiAlO_2 + 2Al_2O_3 \text{ (film)} \rightleftharpoons LiAl_5O_8. \quad (10)$$

Thus $LiAl_5O_8$ could start to react with aluminium liquid, resulting in a cyclic directed melt oxidation reaction sequence similar to that outlined above.

Conclusions

Composite Al_2O_3/Al ceramics have been obtained by directed melt oxidation of pure aluminium externally doped with a Li source (Li_2CO_3). Products have been produced by directed melt oxidation into both free space and particulate preforms comprising pure α-Al_2O_3. As no other dopants were present, Li can initiate directed oxidation reactions and is therefore an effective dopant for the production of Al_2O_3 from Al by directed melt oxidation.

With Li the directed melt oxidation process was initiated by the formation of $LiAl_5O_8$, which aids the breakdown of the stable oxide film that would normally form on aluminium. Subsequently the process involves motion of Li from within the growth to the reaction front; this can occur because of the high vapour pressure of Li at the reaction temperature. Thus, a Li-containing non-protective lithium aluminate layer was formed on the outward surface of product growth. This layer was instrumental in developing the subsequent cyclic reaction sequence in a similar fashion to the Mg-doped directed oxidation system.

Acknowledgement

This work was undertaken whilst one of us (X.G.) was in receipt of a Sheffield University Scholarship.

References

1. Newkirk, M. S., Urquhart, A. W. & Zwicker, H. R., Formation of lanxide ceramic composite materials. *J. Mater. Res.*, **1** (1986) 81–9.
2. Nagelberg, A. S., Observations on the role of Mg and Si in the directed oxidation of Al–Mg–Si alloys. *J. Mater. Res.*, **7** (1992) 265–8.
3. Aghajanian, M. K., Macmillan, N. H., Kennedy, C. R., Luxzcz, S. J. & Roy, R., Properties and microstructures of lanxide Al_2O_3–Al ceramic composite materials. *J. Mater. Sci.*, **24** (1989) 658–70.
4. Xiao, P. & Derby, B., Alumina/aluminum composites formed by the directed oxidation of aluminum using magnesia as a surface dopant. *J. Am. Ceram. Soc.*, **77** (1994) 1961–70.
5. Gu, X. & Hand, R. J., The production of reinforced aluminium/alumina bodies by directed melt oxidation. *J. Eur. Ceram. Soc.*, **15** (1995) 823–31.
6. Lee, J. D., in *Concise Inorganic Chemistry*. D. Van Nostrand Company Ltd, London, 1965, pp. 69–76.
7. Breval, E., Aghajanian, M. K. & Luszcz, S. J., Microstructure and composition of alumina/aluminum

composites made by directed oxidation of aluminum. *J. Am. Ceram. Soc.*, **73** (1990) 2610–14.
8. Ginsberg, H. & Datta, P. K., Dross formation in commercial aluminium and aluminium alloy melts in relation to the oxygen supply. *Aluminium*, **42** (1966) 681–7.
9. Weiranuch, D. A. Jr & Graddy, G. E. Jr, Wetting and corrosion in Al–Mg–Si–O system. In *Proc. Int. Symp. on Advances in Refractories for the Metallurgical Industries*, Winnipeg, Canada, 1987, ed. M. A. J. Figand. Pergamon Press, New York, 1988.
10. Scanans, G. M. & Butler, E. P., Direct observation of oxidation of aluminium and aluminium alloys. In *Proc. 4th Int. Cong. HVEM*, Toulouse, 1975, pp. 341–4.
11. Field, D. J. & Butler, E. P., Liquid metal oxidation of Al–3 wt% Li. In *Aluminum–Lithium Alloy II, Proc. 2nd Int. Aluminum–Lithium Conf.*, AIME, 1983. The Metallurgical Society of AIME, Warrendale, PA, 1983, pp. 667–73.
12. Kouzmichev, L. V., Myzlin, L. Y., Radin, A. Y. & Goopiev, B. D., Oxidation of aluminium/lithium alloys and method of protection. *Tekhnol. Legk. Splavov Nauchno-Tech Byul Vilsa*, **8** (1975) 18–22.
13. Field, D. J., Scamans, G. M. & Butler, E. P., The high temperature oxidation of Al–Li alloy. In *Aluminum–Lithium Alloy II, Pro. 2nd Int. Aluminum–Lithium Conf.*, AIME, 1983. The Metallurgical Society of AIME, Warrendale, PA, 1983, pp. 657–66.
14. Byker, H. J., Eliezer, I., Eliezer, N. & Howald, R. A., Calculation of a phase diagram for the $LiO_{0.5}$–$AlO_{1.5}$ system. *J. Phys. Chem.*, **83** (1979) 2349–55.